nature physics

SUPPLEMENTARY INFORMATION

DOI: 10.1038/NPHYS2790

Direct measurement of the Zak phase in topological Bloch bands

Marcos Atala,[1,†] Monika Aidelsburger,[1,†] Julio T. Barreiro,[1,2]
Dmitry Abanin,[3] Takuya Kitagawa,[3,4] Eugene Demler,[3] Immanuel Bloch[1,2,*]

[1]Fakultät für Physik, Ludwig-Maximilians-Universität, Schellingstr. 4, 80799 Munich, Germany
[2]Max-Planck Institute of Quantum Optics, Hans-Kopfermann Str. 1, 85748 Garching, Germany
[3]Department of Physics, Harvard University, 17 Oxford Str., Cambridge, MA 02138, USA
[4]Rakuten.Inc, Shinagawa Seaside Rakuten Tower, 4-12-3, 140-0002 Tokyo, Japan
[*]To whom correspondence should be addressed; E-mail: immanuel.bloch@mpq.mpg.de
[†]These two authors contributed equally to this work.

S.I Discussion of the Zak phase in the dimerized lattice

In this section we discuss the Bloch wave functions in the SSH model, and calculate the Zak phase of two dimerized configurations of the model. We consider the most general case when not only tunneling but also on-site potentials on sublattices A and B are dimerized (*S1*):

$$\hat{H} = -\sum_n \left(J\hat{a}_n^\dagger \hat{b}_n + J'\hat{a}_n^\dagger \hat{b}_{n-1} + \text{h.c.} \right) + \Delta \sum_n (\hat{a}_n^\dagger \hat{a}_n - \hat{b}_n^\dagger \hat{b}_n). \tag{S.1}$$

The energy bands and eigenstates can be obtained from the eigenvalue equation

$$\begin{bmatrix} \Delta & -\rho_k \\ -\rho_k^* & -\Delta \end{bmatrix} \begin{pmatrix} \alpha_k \\ \beta_k \end{pmatrix} = \tilde{\varepsilon}_k \begin{pmatrix} \alpha_k \\ \beta_k \end{pmatrix}, \tag{S.2}$$

where

$$\rho_k = Je^{ikd/2} + J'e^{-ikd/2} = |\varepsilon_k| e^{i\theta_k}. \tag{S.3}$$

DOI: 10.1038/NPHYS2790

The variable ε_k in the above expression corresponds to the energy of Bloch states in the SSH model ($\Delta = 0$).

S.I.1 Eigenstates

Solving Eq. (S.2), we obtain for the eigenenergies

$$\tilde{\varepsilon}_k = \pm\sqrt{\Delta^2 + \varepsilon_k^2}. \tag{S.4}$$

Following Ref. (*S2*), we require that $\alpha_{k+G} = \alpha_k$ and $\beta_{k+G} = -\beta_k$. The eigenstates in the lower and upper bands which satisfy this condition can be chosen as follows:

$$\begin{aligned} \begin{pmatrix} \alpha_{-,k} \\ \beta_{-,k} \end{pmatrix} &= \begin{pmatrix} \sin\frac{\gamma_k}{2} \\ \cos\frac{\gamma_k}{2} e^{-i\theta_k} \end{pmatrix} \\ \begin{pmatrix} \alpha_{+,k} \\ \beta_{+,k} \end{pmatrix} &= \begin{pmatrix} -\cos\frac{\gamma_k}{2} \\ \sin\frac{\gamma_k}{2} e^{-i\theta_k} \end{pmatrix}, \end{aligned} \tag{S.5}$$

where γ_k and θ_k are given by (the expression for θ_k is obtained from Eq. (S.3))

$$\begin{aligned} \gamma_k &= \arctan\frac{\varepsilon_k}{\Delta} \\ \theta_k &= \arctan\frac{(J - J')\sin(kd/2)}{(J + J')\cos(kd/2)}. \end{aligned}$$

S.I.2 Zak phase

Generally, the Zak phase for a given band is given by

$$\varphi_{\mathrm{Zak}} = i\int_{-G/2}^{G/2} (\alpha_k^*\partial_k\alpha_k + \beta_k^*\partial_k\beta_k)dk. \tag{S.6}$$

For the wave functions in Eq. (S.5), this gives

$$\begin{aligned} \varphi_{\mathrm{Zak},-}(\Delta) &= \int_{-G/2}^{G/2} \cos^2\frac{\gamma_k}{2}\partial_k\theta_k\, dk, \\ \varphi_{\mathrm{Zak},+}(\Delta) &= \int_{-G/2}^{G/2} \sin^2\frac{\gamma_k}{2}\partial_k\theta_k\, dk. \end{aligned} \tag{S.7}$$

These equations were used to make the green theoretical curve in Fig. 4 of the main text.

For the SSH model $\Delta = 0$ such that $\cos^2 \gamma_k/2 = \sin^2 \gamma_k/2 = 1/2$ and the Zak phases reduce to $\varphi^{\rm D1}_{{\rm Zak},-} = \frac{\pi}{2}$ and $\varphi^{\rm D2}_{{\rm Zak},+} = -\frac{\pi}{2}$.

S.II Zak phase and the choice of a unit cell

We emphasize that the Zak phase, in general, depends on the choice of unit cell for the crystal. Here we would like to clarify why for our choice of the unit cell of the SSH model the Zak phases are given by $\pm\pi/2$ (rather than by 0 or π, as in some previous papers, e.g., see Ref. (*S3*) and references therein).

To understand the relation of the Zak phase to the choice of the unit cell, we first note that the function $u_k(x)$ is not periodic under a translation by a reciprocal lattice vector $G = 2\pi/d$, but rather satisfies the following condition (see Ref. (*S2*)):

$$u_{k+G}(x) = e^{-iGx} u_k(x). \tag{S.8}$$

This guarantees that the full Bloch function $\psi_k(x) = e^{ikx} u_k(x)$ is periodic under a translation by a reciprocal lattice vector G.

The Zak phase is defined in terms of the periodic Bloch functions (see Ref. (*S2*)):

$$\varphi_{\rm Zak} = \int_{-G/2}^{G/2} A(k)\, dk, \;\; A(k) = i\langle u_k | \partial_k u_k \rangle, \tag{S.9}$$

where $A(k)$ is the Berry's connection, and the scalar product is defined as $\langle u|v\rangle = \int_0^d u^*(x)v(x)dx$.

Let us now consider a translation by a distance a: $x' = x + a$, which leads to a different choice of the unit cell (unless $a = nd$, where n is integer). The new unit cell is $x' \in [0, d)$, or,

DOI: 10.1038/NPHYS2790

equivalently, $x \in [-a, d-a)$. Then, in order for the condition in Eq. (S.8) to be satisfied, the Bloch functions have to be redefined as follows:

$$u'_k(x') = u_k(x'-a)e^{-ika}. \tag{S.10}$$

The Berry connection is modified accordingly:

$$A'(k) = i\langle u'_k|\partial_k u'_k\rangle = i\langle u_k|\partial_k u_k\rangle + a = A(k) + a.$$

Integrating the Berry connection over the Brillouin zone, we obtain the change in the Zak phase:

$$\varphi'_{\mathrm{Zak}} = \varphi_{\mathrm{Zak}} + Ga = \varphi_Z + 2\pi a/d. \tag{S.11}$$

The Zak phase changes by 2π under a translation by a multiple of the lattice vector d. Thus it is not surprising that our choice of the unit cell for the SSH model gives rise to the values of the Zak phase which are different from the values mentioned in some other works (*S3*). The difference of $\pi/2$ appears due to the shift of the unit cell by $a = d/4$.

We also emphasize that, even though the Zak phase itself depends on the choice of the unit cell, the difference of the Zak phases in two states, measured in our experiment, is an invariant which describes the topological properties of the two states (see Ref. (*S4*)).

S.III Bloch oscillations in superlattices

Here we derive the dynamical equations for the Bloch oscillations in the dimerized lattice. We consider a dimerized lattice subject to an external force, described by the Hamiltonian

$$\hat{H}_F = \hat{H} - F\sum_n \left\{ (x_n - x_0)\hat{a}_n^\dagger \hat{a}_n + (x_n + \frac{d}{2} - x_0)\hat{b}_n^\dagger \hat{b}_n \right\}$$

with $x_n = nd$. For simplicity, we wrote this equation for only one of the pseudo-spin species; an equation for the dynamics of other pseudo-spin is obtained by a substitution $F \to -F$ in

the above equation. Slowly fluctuating magnetic fields in our experiment will add an extra Zeeman energy difference between two pseudo-spins, which can be absorbed in the definition of x_0.

Eigenstates of $\hat{H}_F$ are plane waves with energies $\pm\tilde{\varepsilon}_k = \pm\sqrt{\Delta^2+\varepsilon_k^2}$. For our analysis it is convenient to work in second quantization,

$$\hat{c}^\dagger_{\pm,k} = \frac{1}{\sqrt{N}}\sum_n \left\{\alpha_{\pm,k}e^{ikx_n}\hat{a}^\dagger_n + \beta_{\pm,k}e^{ik(x_n+\frac{d}{2})}\hat{b}^\dagger_n\right\} \tag{S.12}$$

where N is the total number of sites in the lattice. For finite F we need to solve the Heisenberg equation of motion $\frac{d}{dt}\hat{\Psi}^\dagger(t) = \frac{i}{\hbar}[\hat{H}_F, \hat{\Psi}^\dagger(t)]$. We look for solutions where the quasimomentum changes at a constant rate,

$$\hat{\Psi}^\dagger(t) = A(t)\hat{c}^\dagger_{-,k_0-vt} + B(t)\hat{c}^\dagger_{+,k_0-vt}. \tag{S.13}$$

Using

$$\begin{aligned}\frac{\partial}{\partial t}\hat{c}^\dagger_{-,k_0-vt} =& -\frac{v}{\sqrt{N}}\sum_n\left[i\alpha_{-,k}x_n + \frac{\partial\alpha_{-,k}}{\partial k}\right]e^{ikx_n}\hat{a}^\dagger_n\ |_{k=k_0-vt}\\ &-\frac{v}{\sqrt{N}}\sum_n\left[i\beta_{-,k}(x_n+\frac{d}{2}) + \frac{\partial\beta_{-,k}}{\partial k}\right]e^{ik(x_n+\frac{1}{2})}\hat{b}^\dagger_n\ |_{k=k_0-vt}\end{aligned}$$

and

$$\begin{aligned}[\hat{H},\hat{c}^\dagger_{-,q}] =& \varepsilon_{-,q}\hat{c}^\dagger_{-,q} - \frac{F}{\sqrt{N}}\sum_n\Big[\alpha_{-,q}(x_n-x_0)e^{iqx_n}\hat{a}^\dagger_n\\ &+\beta_{-,q}(x_n+\frac{d}{2}-x_0)e^{iq(x_n+\frac{d}{2})}\hat{b}^\dagger_n\Big],\end{aligned}$$

we find that the Ansatz in Eq. (S.13) provides a solution of the Heisenberg equation of motion when $v = f = F/\hbar$ and

$$\begin{aligned}-i\dot{A} =& \varepsilon_{-,k_0-ft}A/\hbar + fx_0A - \frac{fA}{i}\langle u_{-,k_0-ft}|\partial_k u_{-,k_0-ft}\rangle\\ &-\frac{fB}{i}\langle u_{-,k_0-ft}|\partial_k u_{+,k_0-ft}\rangle\end{aligned} \tag{S.14}$$

DOI: 10.1038/NPHYS2790

and a similar equation for B. The last term in Eq. (S.14) describes non-adiabatic mixing of the bands, which we neglect. Assuming that atoms occupy only the lower band ($B = 0$ and $|A| = 1$) and taking $A(t) = e^{i\varphi(t)}$, we obtain:

$$\dot{\varphi} = \varepsilon_{-,k_0-ft}/\hbar + fx_0 - \frac{f}{i}\langle u_{-,k_0-ft}|\partial_k u_{-,k_0-ft}\rangle. \tag{S.15}$$

The first term in Eq. (S.15) describes the dynamical phase contribution, the second is, effectively, the Zeeman phase (which contains the effect of the fluctuating magnetic fields that shift x_0), and the last term describes the Berry's phase part. Integrating Eq. (S.15) over a period of the Bloch oscillations gives Eq. (3) of the main text, with $\varphi_{\text{Zeeman}} = \pm fx_0 t$, where $\pm$ sign corresponds to the two pseudo-spin species.

A crucial point is that our spin-echo type protocol is insensitive to both the Zeeman phase (or, equivalently, to the value of x_0) and the dynamical phase. The spin-echo nature of the experiment guarantees that the Zeeman phases for the two trajectories are equal (each atom spends half of the time in the spin-up state, and half of the time in the spin-down state). The dynamical phases acquired during the motion in the Bloch bands cancel out due to the reflection symmetry of the dispersion relation, $\varepsilon_k = \varepsilon_{-k}$. Both of these points finally allow us to single out the Zak phase.

S.IV Experimental Sequence

The experimental sequence started by loading in 200 ms a Bose-Einstein condensate of about 5×10^4 atoms in the Zeeman state $|F = 1, m_F = -1\rangle = |\downarrow\rangle$ into a dimerized 1D lattice of $V_l = 13E_{r,l}$, $V_s = 4E_{r,s}$ and $\phi = 0$, where $E_{r,i} = h^2/2m\lambda_i$, $i = l, s$. Thereafter, a magnetic field gradient of $f = 1.18(4)$ kHz$/d$ was ramped up in 1.5 ms, and subsequently a 3-μs MW $\pi/2$-pulse coupling to the Zeeman state $|F = 2, m_F = -1\rangle = |\uparrow\rangle$ was applied. After half a

Bloch oscillation, when the atoms were at the edge of the band, a π-pulse was applied and the dimerization was swapped (See section Dimerization swap). After an additional time of $425\,\mu$s the atoms returned to $k = 0$ and a final $\pi/2$-pulse with a phase φ_{MW} was applied. At the end of the sequence we measured the population fraction of each of the two spin components by using time-of-flight imaging with a Stern-Gerlach gradient field applied during the expansion to separate the different Zeeman states.

The use of different hyperfine states gives, in principle, also a different light shift, and therefore both spin components see a slightly different lattice potential. This difference affects only the cancellation of the dynamical phases during the Bloch oscillation but not the geometrical phase that they pick up because it is independent of the strength of the lattice. A calculation of the dynamical phases for both spin components shows that the effect, however, is negligible for our experimental parameters.

For the 850-μs Bloch oscillation time and $J/J' = 1$ kHz$/0.06$ kHz, a negligible fraction of atoms was transferred to the upper band because of non-adiabatic Landau-Zener transitions at the band edge. This underlines the adiabaticity of the Bloch oscillations.

Due to a reproducible 80-kHz drift in the offset magnetic field during the time of a full Bloch oscillation, the three MW pulses were not all on resonance. The first (last) $\pi/2$-pulse was detuned by -40 kHz (40 kHz) and the intermediate π-pulse was on resonance, while the coupling strength was about 80 kHz and the Fourier-transform limited linewidth of the resonance was $150(20)$ kHz. This detuning leads to a reduced maximum contrast of the Ramsey fringes of $0.8(1)$. Additionally, the drift in the offset magnetic field adds a constant value to the Zeeman phase φ_{Zeeman}, which is independent of the change in dimerization/staggering, therefore it does

DOI: 10.1038/NPHYS2790

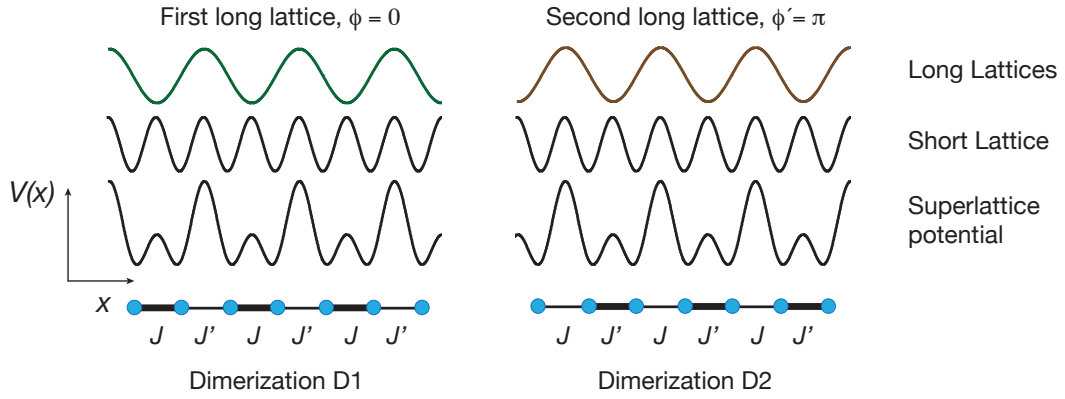

Figure S1: Left (right): Superlattice potential created by using the first (second) long lattice with a phase $\phi = 0$ ($\phi' = \pi$). The corresponding dimerization is $D1$ ($D2$).

not affect the phase difference $\delta\varphi$.

S.V Dimerization swap

In order to change the dimerization from $D1$ to $D2$ we employed a second long lattice, whose amplitude and relative phase ϕ' can be independently controlled. The dimerization exchange was performed by quickly switching off the first long lattice with phase $\phi = 0$ and a ramp-up of the second long lattice with a phase $\phi' = \pi$ within $10\ \mu$s. As the dimerization swap time is much shorter than the Bloch oscillation time, the dimerization exchange can be considered instantaneous and therefore it does not introduce any dynamical phase. The absence of extra dynamical phases when exchanging the long standing wave is also confirmed in Fig. 4 at the point $\Delta = 0$. There, the two superlattices are exchanged, but with the same relative phase respect to the short lattice. As can be seen, the phase difference between the Ramsey fringes is zero, confirming that there is no additional phase induced by the swap of the long lattices. The resulting lattice potentials of the different lattice configurations are shown in Fig. S1, corresponding to the two dimerizations of the SSH model.

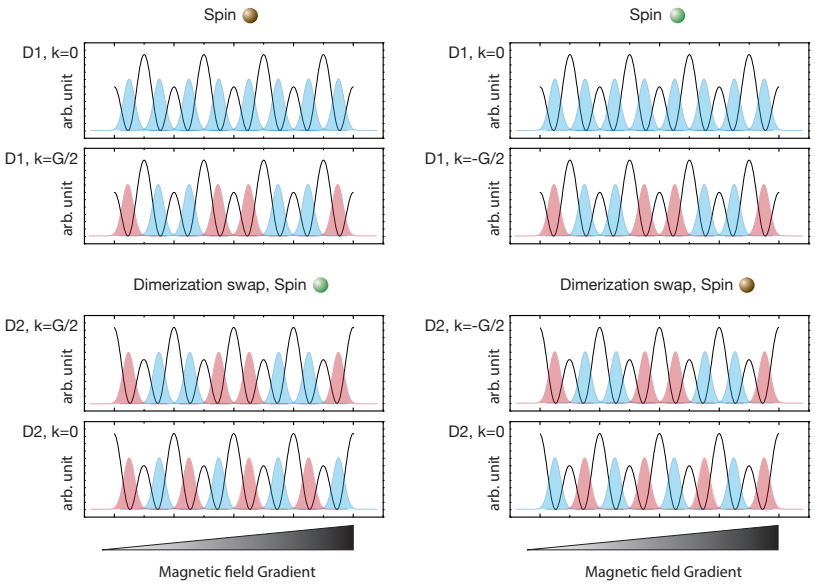

Figure S2: Left (right): Bloch function evolution during the experimental sequence for the component initially in spin-up (-down) state. The solid back lines denote the superlattice potential in arbitrary units as a function of position along the lattice (horizontal axis). Red (blue) color denotes positive (negative) sign of the wavefunction. Initially the Bloch function is symmetric inside the double well, and it is the same for every double well. After the first part of the Bloch oscillation it reaches $k = G/2(-G/2)$ and the wave function is symmetric inside each double well, and it alternates in sign from one double well to the next. The two spin components also have an additional geometrical phase equal to $\pi/4$ which is not displayed in the figure. A sudden dimerization swap shifts the potential by one lattice site, leaving the wave function unperturbed and projecting it into the upper band. Simultaneously the MW pulse flips the spins. After the second part of the Bloch oscillation the two spin components return to $k = 0$ in the upper band, but with opposite signs.

S.VI Alternative interpretation of the experimental scheme

One can explain the Zak phase acquired by the wave functions when completing the experimental sequence by looking at the evolution of the Bloch wave functions. Initially the Bloch wave function is homogeneous and has the same sign on each double well, and the corresponding Wannier functions are symmetric (see Fig. S2). After the first part of the Bloch oscillation, one spin component is at $k = G/2$ and the other at $k = -G/2$ and the corresponding Wannier

DOI: 10.1038/NPHYS2790

functions are again symmetric. Additionally, the wave function sign alternates from one double well to the next one and there is a geometrical phase between the two spin components equal to $\pi/4$. The dimerization swap projects the wave function in the upper band of the system with dimerization $D2$, which at $k = \pm G/2$ has antisymmetric Wannier functions and alternates in sign from one double well to the next one. Finally, after the second part of the Bloch oscillation, both components return to $k = 0$ in the upper band and they have opposite signs, which reflects the Zak phase equal to π.

S.VII Measuring the Zak phase at $\Delta \neq 0$: projection onto lower and upper bands

Our protocol for measuring the Zak phase at $\Delta \neq 0$, described in the main text, involves a sudden turn on/off of Δ when the atoms, initially in the lower band, reach the edges of the Brillouin zone at $k = \pm\pi/d$. In such a process, a fraction of atoms get excited to the upper band. The upper- and lower-band populations $n_\pm$ after such a non-adiabatic turn on/off of the staggering Δ can be obtained by projecting the lower-band eigenstates in Eq. (S.5) with $\Delta = 0$ onto the states with $\Delta \neq 0$. They are given by

$$n_\pm = \frac{1 \mp \sin\gamma_k}{2} = \frac{\tilde{\varepsilon}_k \mp \varepsilon_k}{2\tilde{\varepsilon}_k}. \tag{S.16}$$

In the above expression, all quantities are defined for the final non-zero value of Δ.

S.VIII Extracting the phase difference $\varphi_{\rm Zak} - \varphi_{\rm Zak}(\Delta)$ from the measured Ramsey fringes

In this section we explain how we extract the value of $\varphi_{\rm Zak} - \varphi_{\rm Zak}(\Delta)$ from the measured fringes for Fig. 4 of the main text. Due to a fraction of atoms transferred to the upper band when $\Delta \neq 0$, the phase difference between the two Ramsey fringes deviates from $\varphi_{\rm Zak} - \varphi_{\rm Zak}(\Delta)$. The rea-

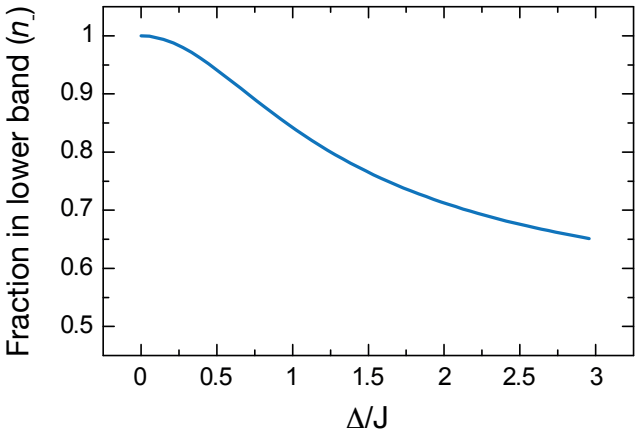

Figure S3: Atom fraction in the lower band (n_-) as a function of the energy offset in units of J. As Δ/J increases the fraction transferred to the upper band (n_+) also increases. In the limit $\Delta/J \to \infty, n_- \to 0.5$

son for this is that the fraction of atoms in the upper band acquires a different geometric phase $\varphi_{\mathrm{Zak},+}(\Delta) = \pi - \varphi_{\mathrm{Zak},-}(\Delta)$ (see Eq. (S.7)) than the fraction in the lower band. Therefore, when measuring the Ramsey fringe, both phases enter into play as explained below.

As described in the main text, for half of the measured points during the first part of the Bloch oscillation, the atoms evolve in the lower band of the dimerized system with $\Delta = 0$ (for the second half of the measured points the atoms start in the lower band with $\Delta \neq 0$, which gives essentially the same result). When they reach the edge of the band, the wave function is

$$|\psi\rangle = \frac{1}{\sqrt{2}}\left(|\uparrow, -G/2\rangle_- e^{i\varphi_{\mathrm{Zak}}/2} + |\downarrow, G/2\rangle_- e^{-i\varphi_{\mathrm{Zak}}/2}\right),$$

where $\varphi_{\mathrm{Zak}} = \varphi_{\mathrm{Zak},-}(\Delta = 0)$. When the MW π-pulse is applied and the energy offset Δ is quickly introduced, the spins are flipped and the population in the bands are $n_\pm$ (see Eq. (S.16)

DOI: 10.1038/NPHYS2790

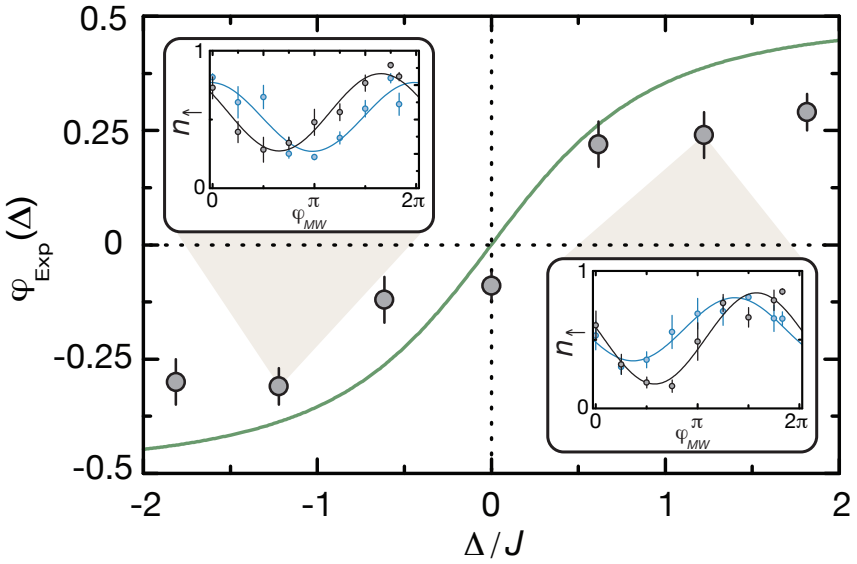

Figure S4: Measured phase difference φ_{Exp} as a function of the energy offset in units of J. The green line shows the predicted value of $\varphi_{\rm Zak} - \varphi_{\rm Zak}(\Delta)$ when there is no population transfer to the upper band.

and Fig. S3):

$$|\psi\rangle = \frac{1}{\sqrt{2}}\Big(\sqrt{n_-}|-G/2\rangle_- + \sqrt{n_+}|-G/2\rangle_+\Big)e^{i\varphi_{\rm Zak}/2}|\downarrow\rangle + \frac{1}{\sqrt{2}}\Big(\sqrt{n_-}|G/2\rangle_- + \sqrt{n_+}|G/2\rangle_+\Big)e^{-i\varphi_{\rm Zak}/2}|\uparrow\rangle.$$

In the second half of the Bloch oscillation the particles return to $k = 0$ and the fraction in the upper (lower) band picks up a phase $\varphi_{\rm Zak,+}(\Delta)$ ($\varphi_{\rm Zak,-}(\Delta)$), such that the resulting state vector is:

$$|\psi\rangle = \frac{1}{\sqrt{2}}\left\{\sqrt{n_-}|0\rangle_- e^{-i\varphi_{\rm Zak,-}(\Delta)/2} + \sqrt{n_+}|0\rangle_+ e^{-i\varphi_{\rm Zak,+}(\Delta)/2}\right\} e^{i\varphi_{\rm Zak}/2}|\downarrow\rangle + \frac{1}{\sqrt{2}}\left\{\sqrt{n_-}|0\rangle_- e^{i\varphi_{Zak,-}(\Delta)/2} + \sqrt{n_+}|0\rangle_+ e^{i\varphi_{Zak,+}(\Delta)/2}\right\} e^{-i\varphi_{\rm Zak}/2}|\uparrow\rangle.$$

Finally, we apply a $\pi/2$-pulse with a MW phase that rotates the spins to $|\uparrow\rangle \rightarrow \frac{1}{\sqrt{2}}(e^{-\varphi_{MW}/2}|\uparrow\rangle + e^{+\varphi_{MW}/2}|\downarrow\rangle)$ and $|\downarrow\rangle \rightarrow \frac{1}{\sqrt{2}}(e^{\varphi_{MW}/2}|\uparrow\rangle + e^{-\varphi_{MW}/2}|\downarrow\rangle)$. After this pulse, the total population

in $|\uparrow\rangle$ is given by:

$$n_\uparrow = \frac{1}{2}\left\{1 + n_- \cos(\varphi_{\mathrm{Zak}} - \varphi_{\mathrm{Zak},-}(\Delta) + \varphi_{MW}) + n_+ \cos(\varphi_{\mathrm{Zak}} - \varphi_{\mathrm{Zak},+}(\Delta) + \varphi_{MW})\right\}, \tag{S.17}$$

and a similar expression for $n_\downarrow$. The Ramsey fringe is obtained by measuring the population in each spin component as a function of the MW phase φ_{MW}.

For negligible n_+ the phase of the Ramsey fringes directly corresponds to $\varphi_{\mathrm{Zak}} - \varphi_{\mathrm{Zak},-}(\Delta)$. For any finite value of n_+, we can recast Eq. (S.17) in the form $A + B\cos(\varphi_{Exp} + \varphi_{MW})$ and solve for $\varphi_{\mathrm{Zak}} - \varphi_{\mathrm{Zak},-}(\Delta)$ using the relation $\varphi_{\mathrm{Zak},+}(\Delta) = \pi - \varphi_{\mathrm{Zak},-}(\Delta)$ and the theoretical values of $n_\pm$, where φ_{Exp} is the measured phase difference between the Ramsey fringes. The resulting values of $\varphi_{\mathrm{Zak}} - \varphi_{\mathrm{Zak},-}(\Delta)$ are displayed in Fig. 4 of the main text, and the values of φ_{Exp} are shown in Fig. S4.

S.IX Symmetries and generalizations of the measurement scheme

The reader might be concerned that the scheme implemented in our experiment requires special symmetries and could be restricted to two-band models. First, the use of the spin-echo protocol and of the second band was the simplest way to address the problem of fluctuating magnetic fields in the laboratory. In principle, the scheme does not require the use of a second band, if sufficiently stable magnetic fields are achieved. Then the Ramsey sequence can be closed after Bloch oscillations to the edges of *a single band* (see Step 1 of our protocol). In such a case the dynamical phase would be cancelled for any time-reversal invariant Hamiltonian. Second, in the absence of any symmetry in the band, the dynamical phase could be still isolated from the geometric phase by analyzing the Ramsey phase as a function of the Bloch oscillation velocity.

We also would like to note that while the Ramsey fringe only measures the Zak phase mod-

DOI: 10.1038/NPHYS2790

ulo 2π, a complete characterization can be achieved by evolving from a reference Hamiltonian into a desired Hamiltonian without closing a gap in the energy spectrum and monitoring the evolution of the Zak phase.

S.X Edge states and its relation to the Zak phase - Trap effects

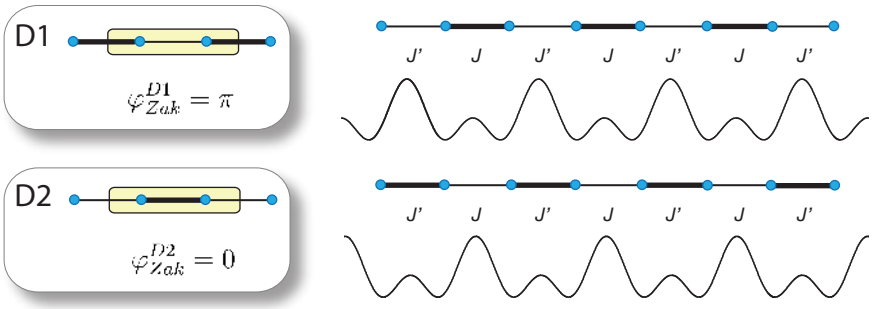

Figure S5: Schematics of the mirror centered dimerizations D1 and D2 and the corresponding lattice potentials for a finite size system. For this choice of the unit cell, the two topological distinct phases D1 and D2 give a value for the Zak phase of π and 0 respectively.

The Zak phase (divided by π) can indeed assume the same meaning as the Chern number to indicate topologically trivial or non-trivial phases without and with edge states present. This can best be seen for a mirror symmetric choice of unit cell in the SSH model (different from the one chosen in the manuscript, see Fig. S5). For such a choice, the Zak phase assumes values of π or 0 for the two dimerized phases D1 and D2. A finite-size system (composed of an integer number of unit cells), then shows no edge states (topologically trivial) for $\varphi_{Zak} = 0$ or two edge states (topologically non-trivial) for $\varphi_{Zak} = \pi$. In general, one can say that the phase difference $\varphi_{Zak}^{D1} - \varphi_{Zak}^{D2} = \pi$ indicates that the system contains trivial and non-trivial topological phases.

When a power law potential $(r/r_0)^\gamma$ is present, we find the absence or presence of edge states to be still clearly visible down to power laws of about $\gamma = 10 - 12$ compared to the ideal

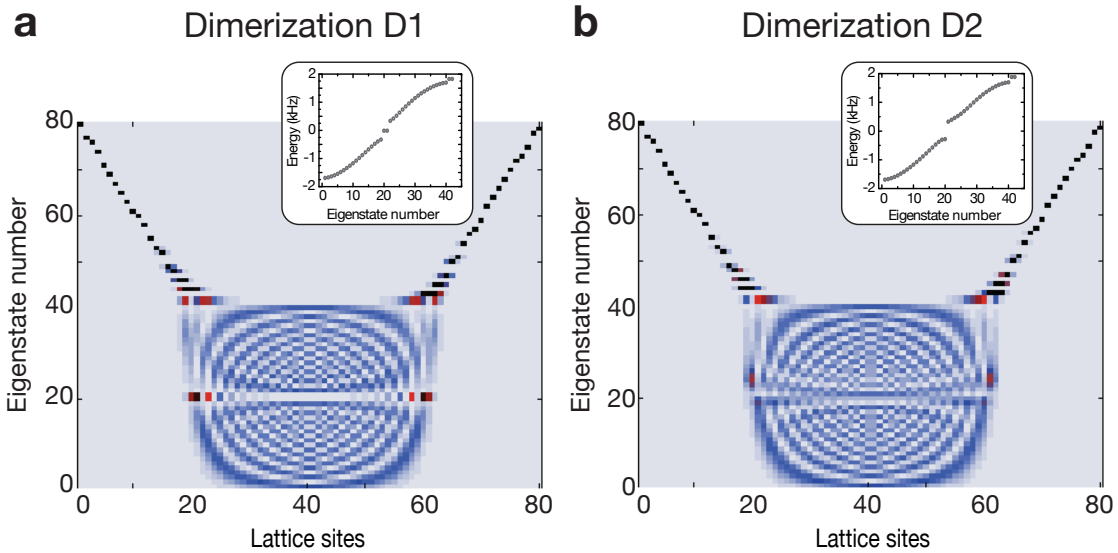

Figure S6: Density plot for the different eigenstates for the dimerizations D1 (**a**) and D2 (**b**) in a finite size system with 80 lattice sites, coupling $J/J' = 1\text{kHz}/0.7\text{kHz}$ and trapping potential of the form $(r/r_0)^\gamma$ with $\gamma = 12$ and $r_0 = 20$ lattice sites. The horizontal axis represents the lattice sites and the vertical axis the eigenstate number. The insets show the energies as a function of the eigenstate number up to 40. For the dimerization D1 there are two isolated eigenenergies that correspond to the two visible localized edge states. For the dimerization D2 there is no isolated eigenstate and there is no visible localized state

box-potential confinement discussed above (see Fig. S6 for $\gamma = 12$). Such system should also clearly allow one to observe charge fractionalization although the edge states spread out over a larger region for lower gamma and will reduce the value of the measured fractional charge (relative to the background density of 1/2 in a half filled band case). Clearly, a situation with hard walls would be favorable for experiments.

References and Notes

S1. M. J. Rice and E. J. Mele. Elementary Excitations of a Linearly Conjugated Diatomic Polymer. Phys. Rev. Lett. 49, 1455-1459 (1982).

S2. J. Zak. Berrys phase for energy bands in solids. Phys. Rev. Lett. 62, 2747-2750 (1989).

DOI: 10.1038/NPHYS2790

S3. P. Delplace, D. Ullmo, G. Montambaux. Zak phase and the existence of edge states in graphene. Phys. Rev. B 84, 195452 (2011).

S4. R. D. King-Smith and D. Vanderbilt. Theory of polarization of crystalline solids. Phys. Rev. B 47, 1651-1654 (1993).